6. Long-term monitoring of atmospheric methane

Lead authors: Douglas Worthy, Carrie Taylor, Ed Dlugokencky, Elton Chan, Euan G. Nisbet, Tuomas Laurila
Contributing authors: Rebecca E. Fisher, James France, David Lowry, Anna Karion, John Miller, Colm Sweeney, James W.C. White

6.1 Introduction

Long-term, systematic measurements of atmospheric methane abundance from a well-calibrated network of air sampling sites are essential to support an assessment of long-term trends, as well as changes in shorter term variability. Measurements are made using sampling strategies that provide information about atmospheric levels over different temporal and spatial scales. Low frequency (i.e. weekly) air samples collected in flasks at remote background sites sample well-mixed air that yields large-scale information about the Arctic region. Continuous measurements are also made at some sites, with the data subsequently averaged to generate a high-frequency (e.g. hourly) time series. Such measurements provide information about the variability in atmospheric methane concentrations, from which information about processes affecting levels at local to regional scales can be determined. When combined with models of atmospheric chemistry and transport, measurements of atmospheric abundance can provide information about methane emissions at larger spatial scales than flux measurements with micrometeorological techniques (see Ch. 3 and 7). Atmospheric methane data provide an important, large-scale perspective to understanding global and regional carbon sources and sinks. As a result of atmospheric transport and mixing, the observed changes in atmospheric concentration reflect large-scale balance or imbalance between emissions and losses (or sinks). Given this relationship, and with sufficient measurement precision and surface coverage (e.g. measurement sites), source region signatures can be inferred.

Further information about emission source type can be obtained from measurements of stable isotopic composition, because methane originating from different sources can have different isotopic signatures.

This chapter summarizes the most recent observations of atmospheric methane from Arctic and sub-Arctic monitoring sites. The objectives of this chapter are to present analysis of available ambient methane observations from a suite of Arctic locations and to highlight how long-term observational data can be used to gain an improved understanding of regional-scale processes and sources affecting methane.

The objectives are targeted in order to answer the science questions posed to the Methane Expert Group, including:

What are the trends and variability in Arctic methane concentrations and what are the primary drivers of this variability?

How much of a trend in atmospheric methane abundance can be detected with the current monitoring network?

Is there evidence of increasing Arctic methane emissions in the atmospheric observations?

This chapter focuses on the long-term systematic measurements of atmospheric methane, and does not address short-term field campaign measurements targeted towards improved understanding of atmospheric processes, nor does it include an analysis of column measurements that provide information on the vertical distribution of methane.

6.2 Surface observations of atmospheric methane

Atmospheric methane monitoring in the Arctic began in the mid-1980s. Analytical instruments used to measure atmospheric methane are calibrated against a common standard scale – the World Meteorological Organization's Global Atmosphere Watch (WMO GAW) methane mole fraction scale – and measurements are reported as dry air mole fractions. Atmospheric methane is measured in nanomoles (billionths of a mole) per mole of dry air and reported as parts per billion (10^9; ppb). (For simplicity, throughout this chapter – and consistent with the rest of this report – methane mole fractions are referred to as methane concentrations or abundances.) Gas chromatography with flame ionization detection has typically been used for analysis of methane in weekly discrete air samples collected in flasks. In addition to gas chromatography, recent technological advances have allowed for higher resolution continuous (hourly) observations, primarily through the incorporation of new multi-species analyzers, including carbon dioxide (CO_2), methane (CH_4) and carbon monoxide (CO), using cavity enhanced absorption spectroscopy techniques such as Cavity Ring Spectroscopy (Crosson 2008) and Off-Axis Integrated Cavity Output Spectroscopy (O'Keefe et al. 1999).

Data compatibility and accuracy are ensured primarily through participation in the WMO GAW program. Three main factors contribute to the uncertainty of a single methane measurement: the reproducibility of the calibration values assigned on the standard gas cylinders used to determine the ambient methane mixing ratios; the time-dependent analytical uncertainty for each measurement; and the standard deviation of each hourly averaged or single flask air sample measurement. These uncertainties are generally quantified by independent laboratories (Andrews et al. 2013). However, the most relevant metrics to assess relative uncertainty among individual laboratories are results reported from ongoing standard gas and real air comparisons (Masarie et al. 2001). Inter-laboratory and methodological comparison exercises provide a mechanism to link many individual network data sets in order to provide a measure of network comparability, and to characterize measurement uncertainty (Masarie et al. 2001; Andrews et al. 2013). The WMO has set a global network comparability target goal for methane of ±2 ppb (WMO 2005). Previously reported results of international laboratory intercomparison activities showed consistent average agreement between participating laboratories to be better than 2 ppb (Worthy et al. 2005).

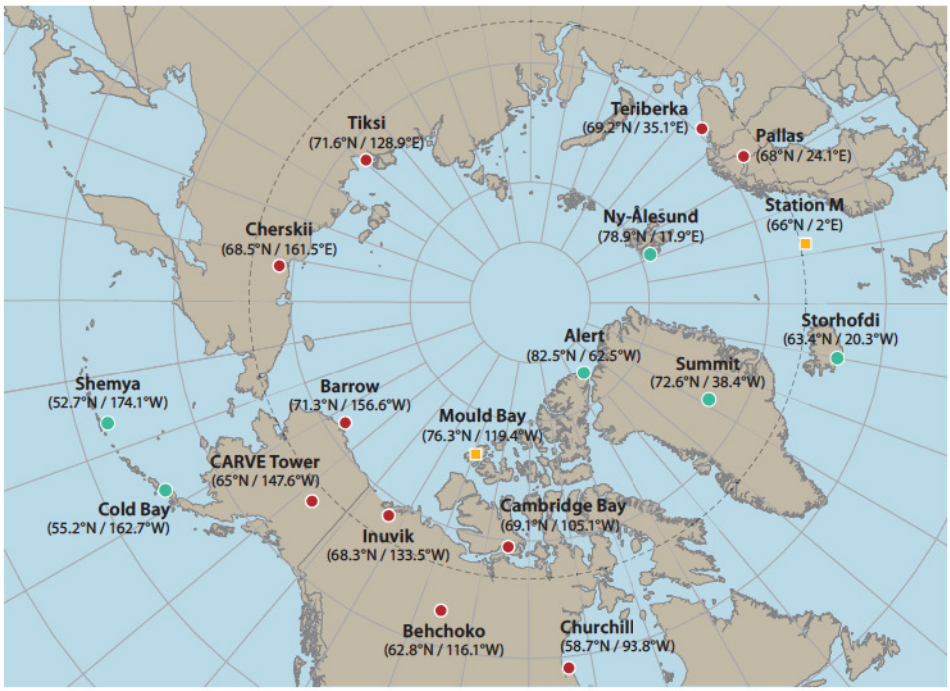

Fig. 6.1 Long-term methane atmospheric monitoring sites in the Arctic and sub-Arctic region (Arctic Circle shown by gray dashed circle at 66.56°N). Remote background sites are shown by green circles; regionally influenced sites are shown by red circles. Air sampling for methane at Mould Bay and Station-M (shown in yellow) stopped in April 1997 and June 2009, respectively.

While the number of sites monitoring atmospheric methane abundance has increased over the past five years, particularly in the Arctic and sub-Arctic regions, the long-term observational network likely remains inadequate to quantitatively characterize polar methane fluxes, given the importance and variety of the potential sources and the vast area of the Arctic. Figure 6.1 shows the sites where multi-year, surface-based discrete (i.e. flask sampled) measurements, continuous measurements, or a combination of both are readily available. The length and continuity of the data record varies from site to site (see Table 6.1). Figure 6.1 and Table 6.1 do not represent the full list of observations potentially available for the Arctic, but rather those stations for which data were available, tied to a common standard and of known quality. Based on these data only, this assessment provides the most comprehensive overview of long-term Arctic atmospheric methane observations currently possible, given the limited number of observing stations in the Arctic.

For the purposes of this study, monitoring sites were characterized as either remote background or regionally influenced. This distinction is for comparative purposes only, and relates primarily to the location of the site relative to source regions. It is also normal that measurements taken at many of

Table 6.1 Summary of available observations of methane in the Arctic.

Station name (Country)	Latitude / Longitude	Height, m above sea level	Sampling History
Alert (Canada)	82.5°N / 62.5°W	210	
Behchoko (Canada)	62.8°N / 116.1°W	179	
Cambridge Bay (Canada)	69.1°N / 105.1°W	38	
Churchill (Canada)	58.7°N / 93.8°W	29	
Inuvik (Canada)	68.3°N / 133.5°W	100	
Mould Bay (Canada)	76.3°N / 119.4°W	30	
Pallas (Finland)	68°N / 24.1°E	560	
Summit (Greenland)	72.6°N / 38.4°W	3238	
Storhofdi (Iceland)	63.4°N / 20.3°W	118	
Ny-Ålesund (Norway)	78.9°N / 11.9°E	474	
Station M (Norway)	66°N / 2°E	0	
Cherskii (Russia)	68.5°N / 161.5°E	30	
Teriberka (Russia)	69.2°N / 35.1°E	40	
Tiksi (Russia)	71.6°N / 128.9°E	8	
Barrow (USA)	71.3°N / 156.6°W	11	
CARVE Tower (USA)	65°N / 147.6°W	611	
Cold Bay (USA)	55.2°N / 162.7°W	21	
Shemya (USA)	52.7°N / 174.1°W	40	

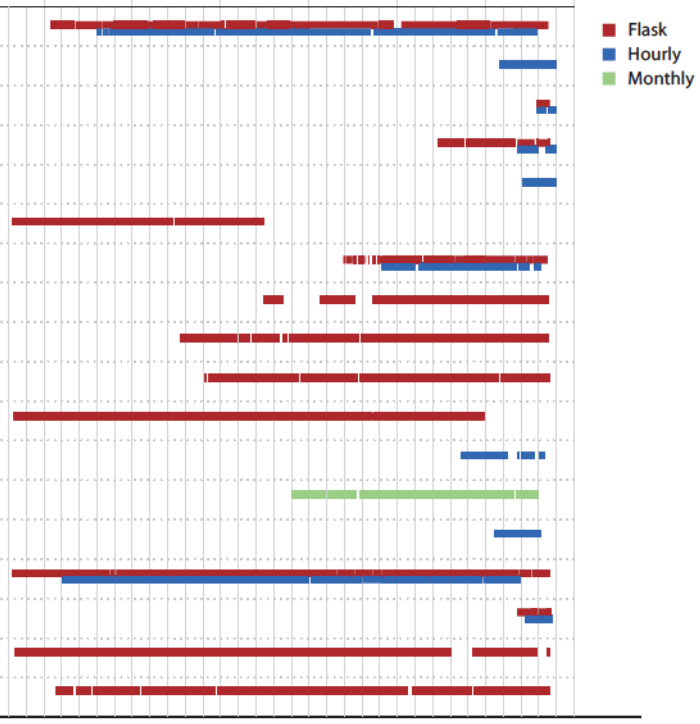

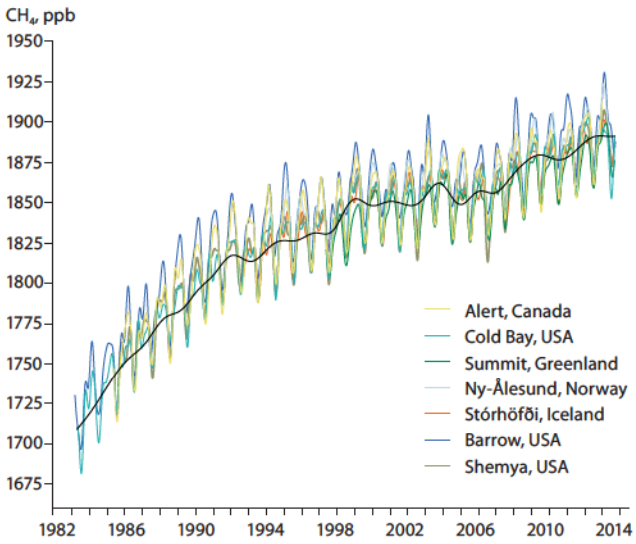

Fig. 6.2 Historical time series of methane concentration at several remote background sites in the Arctic. Smoothed data curves were generated by passing monthly mean methane data through a smoothing function (Nakazawa et al. 1997) for sites starting prior to 1994, with weekly flask samples from NOAA's Cooperative Global Air Sampling Network. For illustrative purposes, the trend, generated using the same smoothing function routine, is shown in black for Alert, Canada.

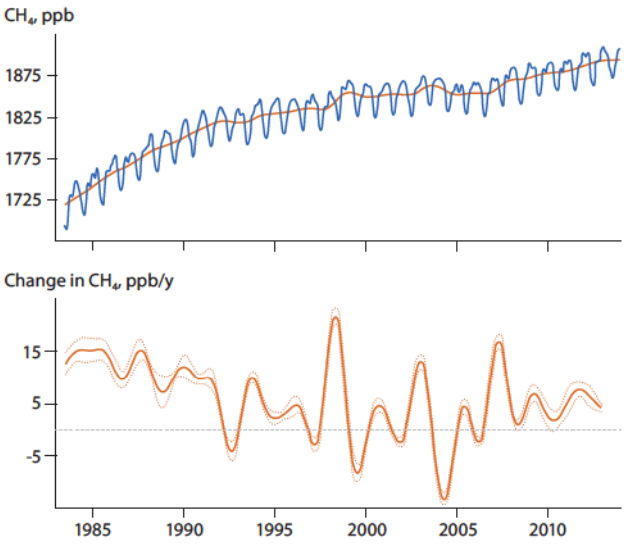

Fig. 6.3 Change in methane abundance at remote background sites within the Arctic. The upper plot shows zonally-averaged (60°–90°N) atmospheric methane concentrations together with the deseasonalized trend, while the lower plot shows the instantaneous methane growth rate determined as the time-derivative of the trend in the upper plot. Zonal means are determined from weekly samples at background sites representing large volumes of well-mixed atmosphere collected as part of the NOAA Cooperative Global Air Sampling Network. Curve-fitting methods are as described by Dlugokencky et al. (2009).

the weekly flask sampling sites reflect background information, because sampling protocols dictate sampling to occur when winds originate from 'clean air' sectors.

Measurements in Arctic locations have been conducted for many decades at remote background sites. These sites are generally coastal, high elevation and relatively far removed from major source regions. An example of extended time series plots for the remote background baseline observatories at Alert (Canada), Cold Bay (USA), Summit (Greenland), Ny-Ålesund (Norway), Storhofdi (Iceland), Barrow (USA) and Shemya (USA) is shown in Fig. 6.2. The smoothed seasonal cycles of methane were derived from the digital filter technique of Nakazawa et al. (1997), using weekly flask samples from NOAA's Cooperative Global Air Sampling Network (Dlugokencky at al. 1994). The near 30-year Arctic record shows an overall increase in methane abundance, consistent with evidence from Arctic and Antarctic ice cores that show a near 300% increase in atmospheric methane concentration since the late 1800s (Etheridge et al. 1992; Blunier et al. 1993). The rate of increase in the atmosphere changed from around 14 ppb/y in the 1980s to near zero over the period from 1999 to 2007. From 2008 to 2013, the observed abundance of methane in the atmosphere has increased annually at around 6 ppb/y (see Sect. 6.3).

6.3 Large-scale trends in Arctic atmospheric methane

Methane emissions mix through the troposphere on time scales that are much shorter than the globally-averaged atmospheric lifetime for methane (9.1±0.9 y; Prather et al. 2012). So, to first order, trends in atmospheric concentration are about the same everywhere on Earth. It is only because of the high quality and inter-laboratory consistency of measurements made by national laboratories that subtle features in zonal averages from smaller regions such as the Arctic can be used to assess temporal changes in emissions. Zonally-averaged dry-air methane abundance at the Earth's surface for the area 60°–90°N determined from remote background sites in NOAA's Cooperative Global Air Sampling Network is shown in Fig. 6.3. The seasonality observed in the graphic has three components: seasonality in methane emissions at a regional scale, seasonality in photochemical methane destruction at the hemispheric scale, and seasonality in the height of the Arctic boundary layer. The trend in methane abundance results from the imbalance between emissions and sinks.

Figure 6.3 also illustrates changes in the atmospheric growth rate over time, showing the instantaneous rate of methane increase, calculated as the time-derivative of the deseasonalized trend. From the start of measurements through to 2006, the atmospheric growth rate decreased from about 14 ppb/y in 1983 to near-zero in 1999/2000, after which a period of interannual variability is evident, with no strong trend observed.

Residuals from a function that approximates the long-term trend and seasonal cycle (2nd-order polynomial and 4 annual harmonics; Thoning et al. 1989) fitted to the methane zonal averages in Fig. 6.3 are plotted in Fig. 6.4. The residuals represent deviations (anomalies) from the long-term behavior. Carbon monoxide is included as it provides additional context on potential sources (i.e. biomass burning) that may affect the long-term trend in atmospheric methane. Changes in the sign of the trend of the residuals in 1992 and 2007 indicate changes in the global methane budget that have affected the trajectory of its future atmospheric burden.

The change observed in 1992 is most likely to have been related to a reduction in anthropogenic emissions from the former Soviet Union (Dlugokencky et al. 1994, 2011; Worthy et al. 2009), and has implications for what may be said about the potential impacts of a warming Arctic on natural emissions.

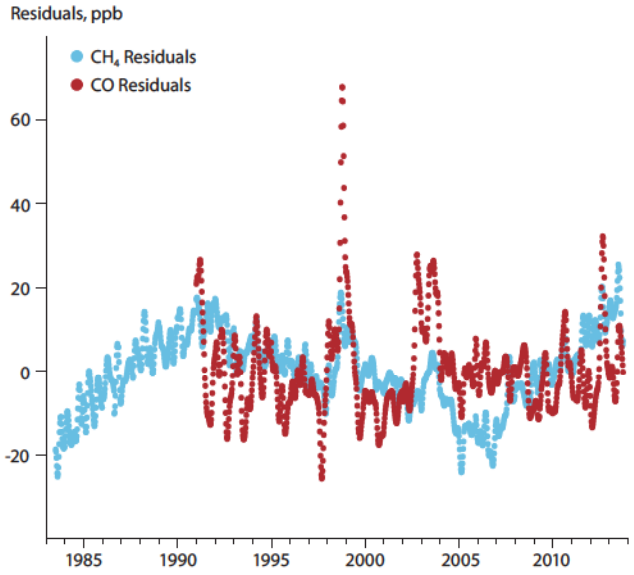

Fig. 6.4 Difference (residuals) between zonal means (53° to 90°N) and function fitted to them that captures mean quadratic trend and seasonal cycle for methane (CH_4) and carbon monoxide (CO) measured in the same samples.

Superimposed on the long-term pattern of atmospheric methane abundance is interannual variability. The main drivers of interannual variability are related to emissions from wetlands and biomass burning (Bousquet et al. 2006), which are affected by large-scale multi-year changes in weather patterns such as the El Niño-Southern Oscillation (ENSO) (Dlugokencky et al. 2009). Specific drivers affecting Arctic methane emissions are surface air and soil temperatures, because the rate of methane production by methanogens is very temperature dependent, with emissions generally increasing with increasing temperature (see Ch. 3). Precipitation amounts can affect the areas and relative wetness of wetlands (wetter conditions generally result in greater emissions, all other parameters the same; see Ch. 3), but they also affect the rate of methane emission from biomass burning, as more burning tends to occur in dry years. The molar ratio of CO to CH_4 for biomass burning is in the range 10 to 20 (Christian et al. 2003), so observations of carbon monoxide are very sensitive to biomass burning. Strong signals from biomass burning at high northern latitudes in 1998, 2002, and 2003 are evident in the CO residuals and are consistent with bottom-up estimates of biomass burning emissions (van der Werf et al. 2006). There may also be contributions to methane anomalies from wetlands.

An anomaly in the Arctic methane time series occurred in 2007 (Fig. 6.4). Atmospheric methane at polar northern latitudes (53°–90°N) increased 13.1±1.3 ppb in 2007, which is greater than the global average increase of 7.9±1.6 ppb (Dlugokencky et al. 2009). Since 2007, Arctic atmospheric methane has been increasing at about the global rate, ~6 ppb/y (2008–2013). The higher annual increase in 2007 in the Arctic, in comparison to the global value, suggests a contribution from Arctic sources, but the magnitude of changes in emissions and attribution to the Arctic region must be understood in the context of atmospheric transport, using a chemical transport model. Arctic emissions mix into a much shallower atmospheric boundary layer than tropical emissions, for example, so relatively large annual increases in Arctic atmospheric methane abundance do not necessarily mean the presence of correspondingly large anomalies in Arctic source emissions (Bousquet et al. 2011). Bergamaschi et al. (2013) found that total methane emissions in the latitude zone 60°–90°N were ~2 Tg CH_4/y greater in 2007 than the average for 2000–2011, but slightly below the average for 2008–2011. Several other studies also found a small increase in Arctic emissions in 2007, consistent with the atmospheric observations (Bousquet et al. 2011; Bruhwiler et al. 2014b).

The Arctic is warming at about twice the global mean rate (see Ch. 1). It is also known that methane emissions from boreal wetlands were a major driver of increased atmospheric methane concentrations in the past (Ch. 3). Therefore, the potential for increased methane emissions from natural sources in the Arctic is an important consideration in evaluating recent changes in methane abundance. Based on measurements of carbon monoxide in the same samples that were measured for methane (Fig. 6.4), the increase in 2007 is not likely to have resulted from biomass burning. Other evidence suggests that changes in the rate of methane loss by reaction with hydroxyl radical (OH) are also not the cause (Dlugokencky et al. 2009). The most likely source contributing to the Arctic increase in 2007 is increased wetland emissions resulting from warmer and wetter than average conditions (Dlugokencky et al. 2009; see also Ch. 3). This scenario is consistent with isotopic measurements (see Sect. 6.6), which show a decrease in $^{13}C_{CH4}$ of methane consistent with wetland emissions. The continued increase since 2007 is likely to have resulted from methane-enriched air transported from lower latitudes, rather than increasing emissions in the Arctic.

Further evidence from the atmospheric observations, which indicates that methane emissions are not detectably increasing at the Arctic scale, is shown in Fig. 6.5, which shows the differences in annual mean methane abundance between northern polar (53°–90°N) and southern polar (53°–90°S) latitudes. From 1984 to 1991, the difference was increasing at 0.4±0.3 ppb/y. Beginning in 1992, a decrease in anthropogenic methane emissions from the former Soviet Union, estimated at 10.6 Tg CH_4/y (Dlugokencky et al. 2003), had a profound effect

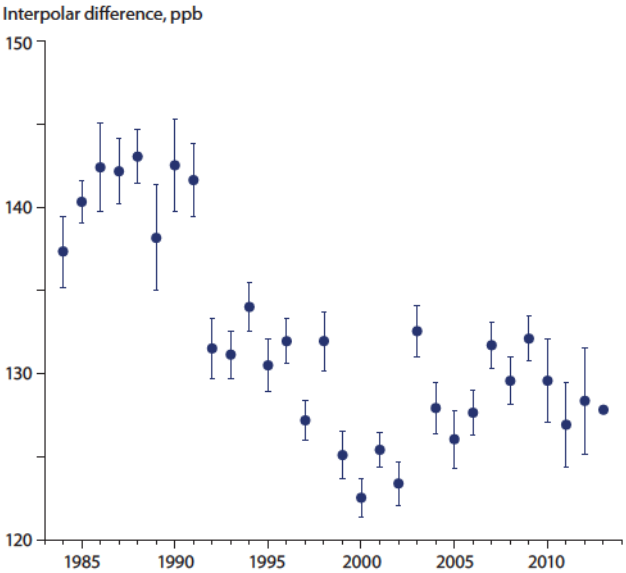

Fig. 6.5 Differences between observed northern polar (53°–90°N) and southern polar (53°–90°S) annual mean methane (CH_4) mole fractions as a function of time. Uncertainties on annual mean differences through 2012 are estimated with a Monte Carlo technique. All uncertainties are 68% confidence intervals.

on the interpolar difference (IPD). Starting in 1992, the trend in IPD reversed sign and was -0.1±0.1 ppb CH_4/y through to 2013. While the IPD varies interannually, it has not returned to the values observed in the late 1980s. Changes in the IPD can potentially provide a sensitive indicator of changes in Arctic methane emissions such as those that may result from changing anthropogenic activity, thawing permafrost, and destabilization of shallow methane hydrates in the marine environment.

6.4 Continuous methane measurements at Arctic locations

This section focusses on data from continuous hourly atmospheric methane measurements at Arctic observation sites to characterize the daily, seasonal and interannual variability in methane concentration. All measurements are directly traceable to the WMO Global Atmosphere Watch X2004 international scale maintained by the Central Calibration Laboratory at NOAA/ESRL in Boulder, Colorado (Dlugokencky et al. 2005).

6.4.1 Diurnal and day-to-day variability

Hourly measurements of methane abundance for 2012 at Inuvik (Canada), Tiksi (Russia) and Cherskii (Russia) – three regionally influenced sites – were chosen to illustrate the observed short-term variability at sites located in the proximity of extensive wetland regions (Fig. 6.6). Also plotted, for reference, are smoothed curves fitted to the methane weekly flask data from the remote background stations at Alert (Canada), Cold Bay (USA), Summit (Greenland) and Ny Ålesund (Norway). The smoothed seasonal cycles were obtained by applying the curve-fitting procedure of Nakazawa et al. (1997) and are included for qualitative comparison with the hourly measurements. Figure 6.6 also includes a magnified view for August 2012, further illustrating the large diurnal and day-to-day variability at regionally influenced sites.

In winter, the observed variability is linked primarily to atmospheric transport from anthropogenic source regions at lower latitudes because natural wetland emissions are lower during winter. Even at sites such as Alert (Canada), located thousands of kilometers from major source regions, the methane time series is frequently highly correlated with other anthropogenic source indicators such as carbon monoxide and black carbon (Worthy et al. 1994). This is particularly the case during well-defined winter episodes that last ~2 to 5 days in duration, and that result from synoptic meteorology, weak vertical mixing and rapid airmass transport originating from Siberian and/or European source regions (Worthy et al. 1994). The episodic events for Inuvik, Tiksi and Cherskii are particularly pronounced relative to events observed at Alert (not shown) due to their closer proximity to anthropogenic source regions. The magnitude of this variability is driven by regional emission strength, local vertical mixing and synoptic conditions.

In summer, short-term variability is much more apparent (relative to winter) and is dominated by diurnal variations. For diurnal variability to occur two conditions must be met: a local flux in methane and physical mixing of the boundary layer that is diurnal. Under strong solar heating during the

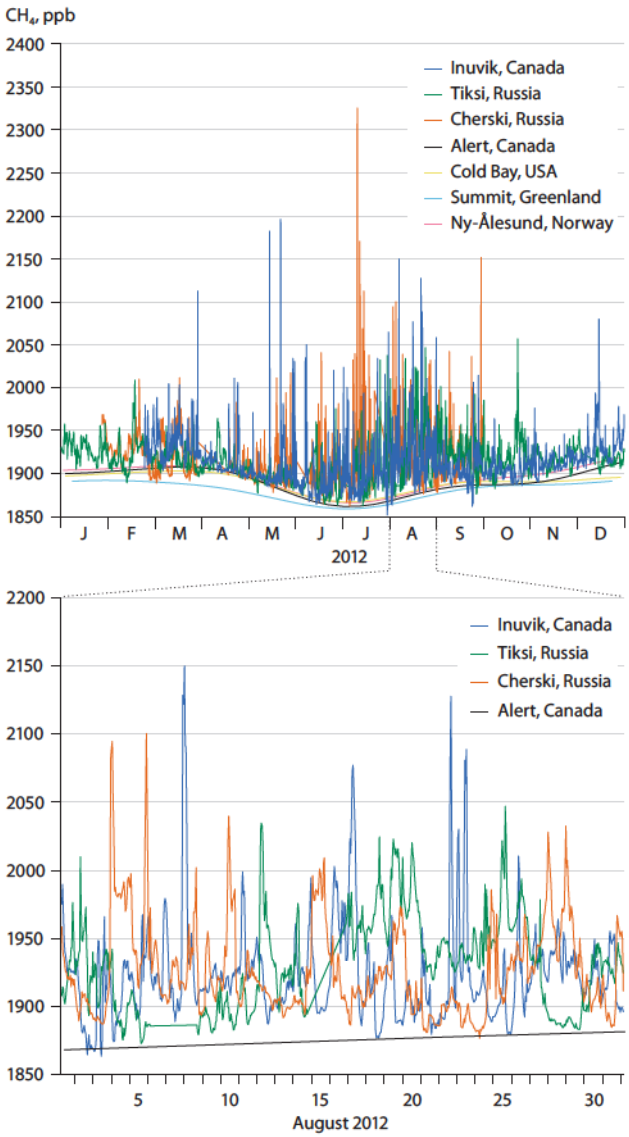

Fig. 6.6 Example of short-term variability in methane abundance at three regionally-influenced sites in the proximity of extensive wetland regions within the Arctic through 2012: Inuvik (Canada), Tiksi (Russia) and Cherski (Russia). Also shown are smooth curves fitted to the methane weekly flask data from four remote background sites: Alert (Canada), Cold Bay (USA), Summit (Greenland) and Ny-Ålesund (Norway). The lower plot shows a magnified window of hourly abundance for August, 2012.

day, the near-surface mixed layer is unstable and generally well mixed throughout the boundary layer. At night, the radiation loss at ground level leads to a cooling of the atmosphere at the surface giving rise to a shallow, stable layer, also known as an inversion. The increase in atmospheric methane during the night is a result of suppressed vertical mixing under this inversion. The magnitude of the nocturnal increase is variable and depends on the depth of the nocturnal inversion and on the regional methane source strength. Owing to enhanced vertical mixing during the day, methane is diluted through the rise of the boundary layer height up to a hundreds of meters or more. In addition, there are also underlying large-scale influences including the regional transport of air masses carrying both anthropogenic and wetland emissions. For example, the hourly data record for Cherskii (Russia) in Fig. 6.6, shows atmospheric methane levels of around 1875 ppb for a three-day period (20–23 August), followed by concentrations greater than 1900 ppb from 24–29 August. Variability of a similar magnitude is evident throughout the monthly time series.

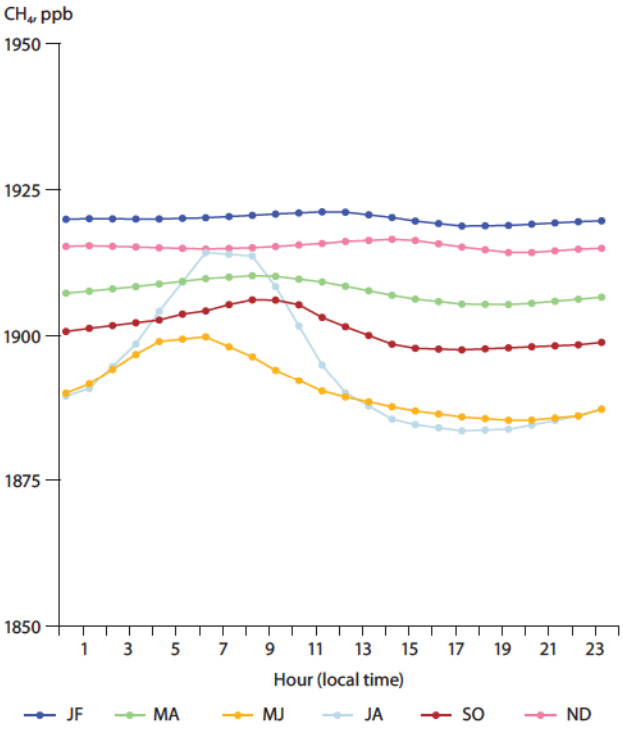

Fig. 6.7 Average diurnal methane cycle at Behchoko (Canada; 62°48'N, 116°93'W) for January/February (JF), March/April (MA), May/June (MJ), July/August (JA), September/October (SO) and November/December (ND), determined from hourly-averaged data from 2011 to 2013.

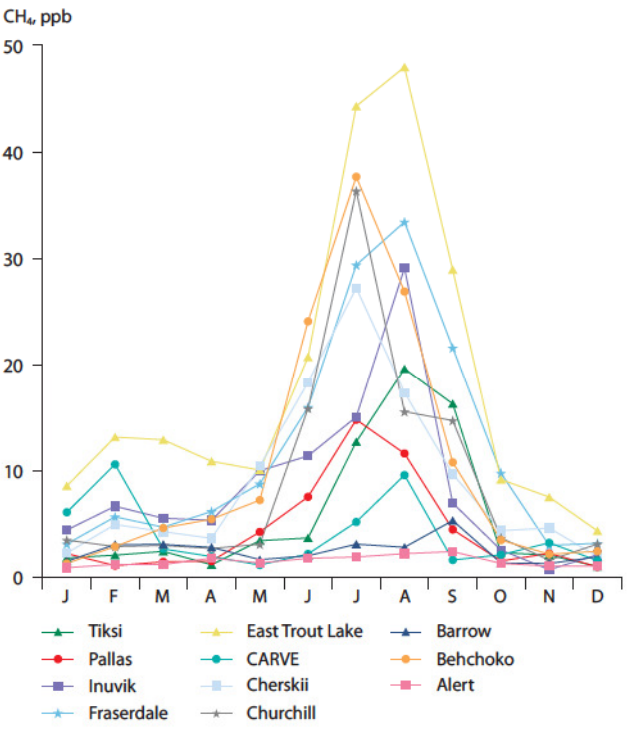

Fig. 6.8 Mean monthly amplitude of the diurnal signal (daily hourly maximum minus same-day hourly minimum), determined from hourly averaged data from 2011 to 2013.

Average diurnal variability throughout the year at Behchoko (Canada) on the northwest tip of Great Slave Lake (see Fig. 6.1) and approximately 80 km northwest of Yellowknife in Canada's Northwest Territories, is shown in Fig. 6.7. The region surrounding Behchoko comprises steep, wooded hills interspersed with numerous lakes and ponds. The mean diurnal methane cycle is shown for two-month average intervals, determined from hourly average data from 2011 to 2013. The average diurnal cycle at Behchoko is strongly seasonally dependent: hardly apparent during winter, beginning to develop in late spring (May/June), reaching a maximum in August when wetland emissions are expected to be elevated, and weakening again in autumn. In summer, methane abundance peaks at around 0600 to 0800 local standard time (LST), owing to methane build-up during the nighttime inversion and then decreases rapidly to reach a minimum at around 1600 to 1800 LST as the boundary layer expands and mixes. As shown in Fig. 6.6, there can be substantial variability in the diurnal cycle from day-to-day. The patterns observed at Behchoko (Canada) are very similar to the diurnal cycle observed at other regionally influenced sites (see Fig. 6.8).

Figure 6.8 shows the amplitude of the diurnal cycle using all available hourly data between 2011 and 2013 for sites listed in Table 6.1, which includes remote background and regionally influenced sites. Also shown, for contrast, are the amplitudes of the diurnal cycle for two lower latitude Canadian sites (Fraserdale and East Trout Lake) located near major natural sources. Fraserdale (49°53'N, 81°34'W) is located on the southern perimeter of the Hudson Bay Lowland (HBL) region, and on the northern edge of the boreal forest. The HBL comprises about 10% of the total area of northern wetlands, and recent studies have estimated the average methane release from the HBL to be ~2 Tg CH_4/y (Pickett-Heaps et al. 2011; Miller et al. 2014). East Trout Lake (54.3°N, 105.0°W) is located in a boreal forest region in western Canada. The terrain contains extensive areas of impeded drainage. Average methane release in summer from wetland regions in western and eastern Canada is similar in magnitude, with estimated fluxes ranging from 20 to 30 mg/m²/day in July and August (Miller et al. 2014).

From November to April, there is very little diurnal variability observed at any site, although there is detectable daily variability (see winter periods in Fig. 6.6). As already noted, much of the daily variability in methane concentration in winter is likely to be due to transport to these sites from anthropogenic source regions at lower latitudes. Diurnal signals are not apparent at any time of the year at the remote background sites of Barrow (USA) and Alert (Canada), strongly indicating either a lack of nearby wetland sources or weak diurnal physical mixing of the boundary layer. In spring and probably soon after the snow melts, nighttime increases in atmospheric methane concentration increase noticeably due to the thawing of the surface soil layer and the subsequent start of wetland activity. Diurnal signals at the regionally influenced sites are greatest in July/August, owing to the probable maximum of wetland methane fluxes at this time of year and the accumulation of methane into a shallower inversion layer at night. The CARVE, Alaska site (64.99°N, 147.60°W) shows the smallest diurnal amplitude, at around 10 ppb. This may be due to relatively low wetland emissions for this region in 2012, but only one year of atmospheric data is currently available. A complicating factor is that the CARVE tower is located on a ridge, several hundred meters higher than its surrounding, and as a result will be less sensitive to local-scale emissions and likely weaker diurnal physical mixing of the boundary layer. For the Arctic located sites, Pallas (Finland) and Behchoko (Canada) show the largest mean diurnal amplitudes, at around 30 ppb.

The diurnal signals start to decrease significantly in September/October, which may be a result of decreased wetland activity, coupled in timing with declining air temperature and thus weaker diurnal physical mixing of the boundary layer and the freezing of the surface soil layer. In High Arctic areas this time of year has been shown, in some years, to coincide with an outburst of methane from wetlands (Mastepanov et al. 2008, 2013), but this phenomenon has not been observed at lower latitudes. At the more southerly sites of Fraserdale and East Trout Lake (Canada), the diurnal signals extend further into autumn, possibly owing to a slightly longer influence from wetland sources (Kuhlmann et al. 1998).

Generally, atmospheric methane measurements at the regionally influenced sites reflect a complex mix of air mass transport from natural and anthropogenic sources, as well as an interaction between the daily cycling of the wetland flux and the vertical mixing dynamics in the atmospheric boundary layer. This is particularly evident during summer when atmospheric methane levels are highly influenced by local and regional wetland emissions and when diurnal cycles are strongest.

6.4.2 Seasonal and interannual variability

From the preceding discussion, it is clear that nighttime methane measurements at sites that observe diurnal signals are not representative of a large, well-mixed volume of the lower troposphere. As a result, nighttime measurements should not be included in the calculation of mean seasonal cycles and trends in methane concentration at regionally influenced sites. Excluding nighttime data is even more important when comparing the mean annual methane cycle at these sites with that at remote background sites. Thus, at the regionally influenced sites, measurements made during the late afternoon (1600 to 1800 LST) – when convective mixing is well developed – are most representative of large spatial scales.

Figure 6.9 compares annual methane cycles at six remote background sites with annual methane cycles at six regionally influenced sites. The characteristics observed during the two-year period are relatively consistent at each of the remote background sites, showing an annual methane cycle with an amplitude of about 55 ppb from the minimum observed in July/August to the maximum observed in February. This is likely to have been driven by the seasonality of methane emissions and sinks in combination with a seasonally variable meridional atmospheric circulation pattern. The high methane levels observed at the remote background sites in winter are due to a negligible OH sink and contributions from long-range transport of polluted air containing methane from anthropogenic emissions at lower latitudes. During spring, methane levels begin to fall due to an increasing OH sink and dilution of northern air masses with air from lower latitudes and aloft containing lower methane concentrations. During summer, the global tropospheric OH sink is strongest, resulting in a minimum in the annual methane cycle in July. By late mid-summer, methane levels begin to increase as the effectiveness of the OH sink decreases and air masses arrive from lower latitudes containing methane from both wetland and anthropogenic emissions. The timing of the annual minimum at the remote background sites can vary from year to year by as much as six weeks, probably due to interannual variability in methane emissions from northern wetlands (Mastepanov et al. 2013).

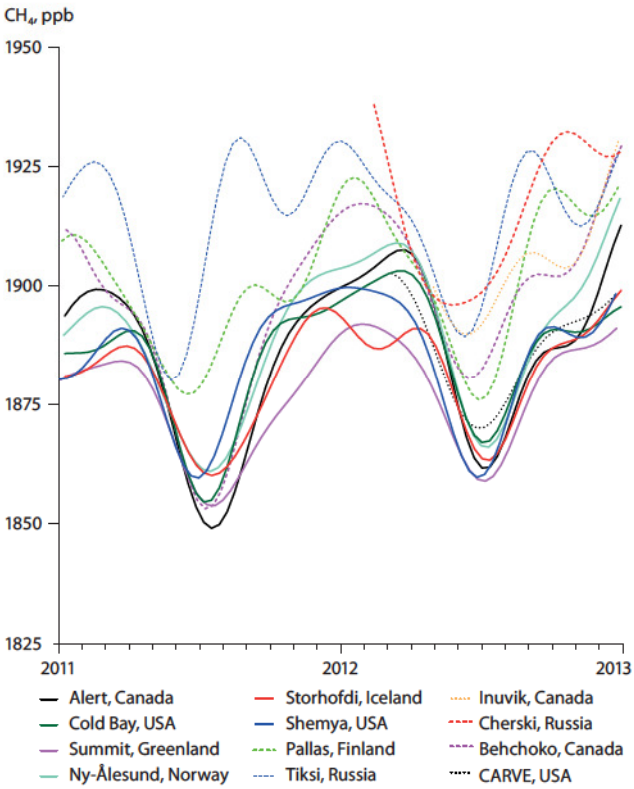

Fig. 6.9 Smoothed seasonal cycles of atmospheric methane concentration for six remote background sites (solid curves) and six regionally influenced sites (dashed curves) through 2011 and 2012. The smoothed seasonal cycles were derived from the digital filter technique of Nakazawa et al. (1997) using weekly discrete air samples for the remote background sites and afternoon hourly-averaged data (1600, 1700 and 1800 LST) for the regionally influenced sites.

The annual methane cycle at the six regionally influenced sites also shows a maximum during winter, but slightly elevated (except for the CARVE site, Alaska) relative to the remote sites, probably due to their closer proximity to anthropogenic source regions. An additional feature in the annual methane cycle of the regionally influenced sites (except for the CARVE site, Alaska), is the presence of a distinct secondary peak in late summer. The magnitude of this secondary peak at these sites relative to the suite of remote background sites varies from site to site and from year to year. Data from the more southerly site at Fraserdale (Ontario, Canada; Worthy et al. 1998) also show a similar secondary peak in summer. This has been shown to be the result of advection of air with enhanced methane levels due to emissions from the extensive wetlands north of Fraserdale, in the Hudson Bay Lowland region, which is a well-documented source of methane (Roulet et al. 1994). It is reasonable to conclude, considering the timing of the summer divergence that the secondary peak observed in mid-summer is predominantly due to the regional influence of wetland emissions. Year-to-year variability in the offset of the regionally influenced sites relative to the remote background sites is probably due to the seasonality in regional wetland methane emissions, atmospheric transport and boundary layer depth.

6.4.3 Trajectory cluster analysis

The observed rise and fall of methane concentrations in the lower atmosphere reflects the transport of methane over long distances, resulting from winds and mixing that take place in the atmosphere. It is possible to infer the magnitude of

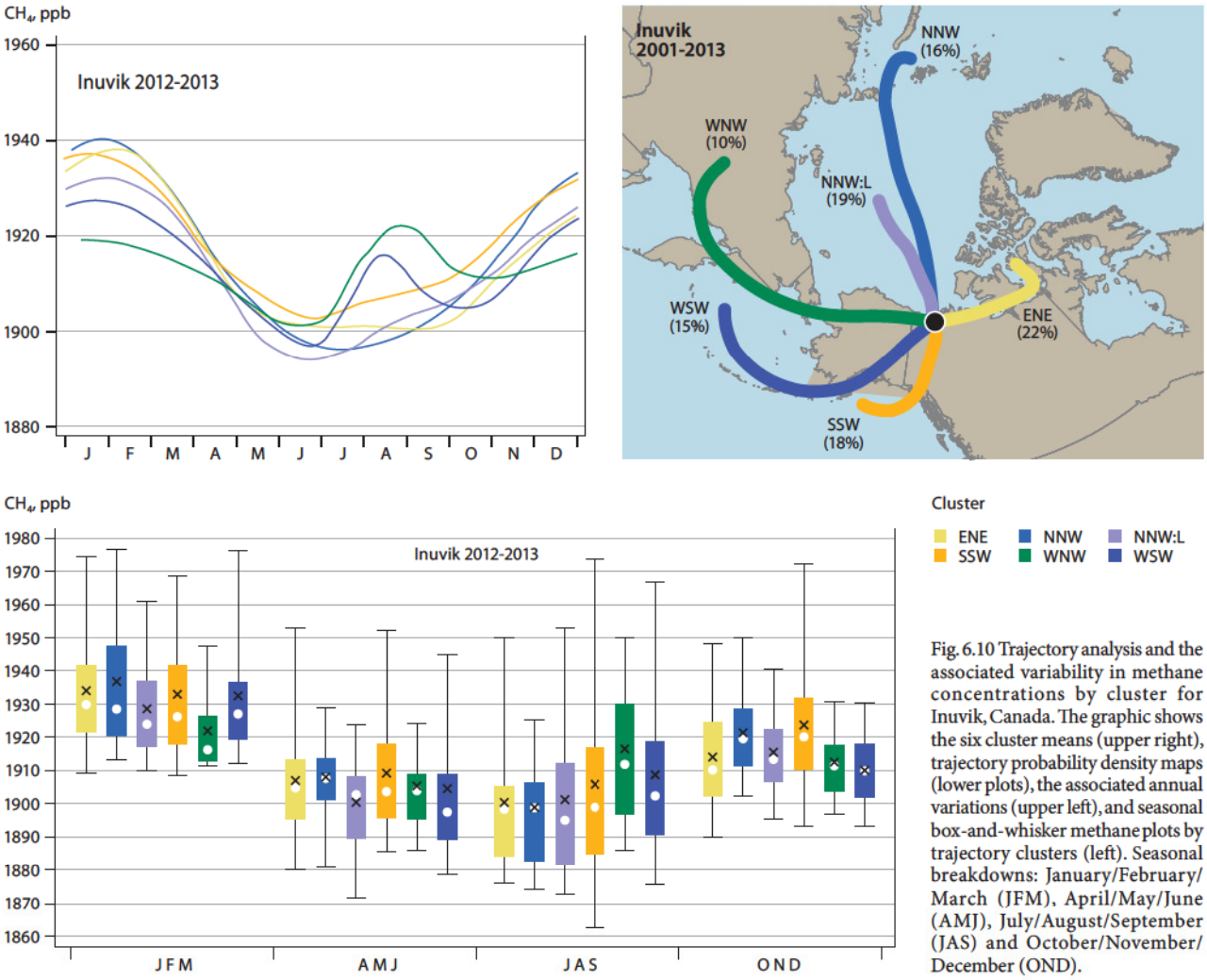

Fig. 6.10 Trajectory analysis and the associated variability in methane concentrations by cluster for Inuvik, Canada. The graphic shows the six cluster means (upper right), trajectory probability density maps (lower plots), the associated annual variations (upper left), and seasonal box-and-whisker methane plots by trajectory clusters (left). Seasonal breakdowns: January/February/March (JFM), April/May/June (AMJ), July/August/September (JAS) and October/November/December (OND).

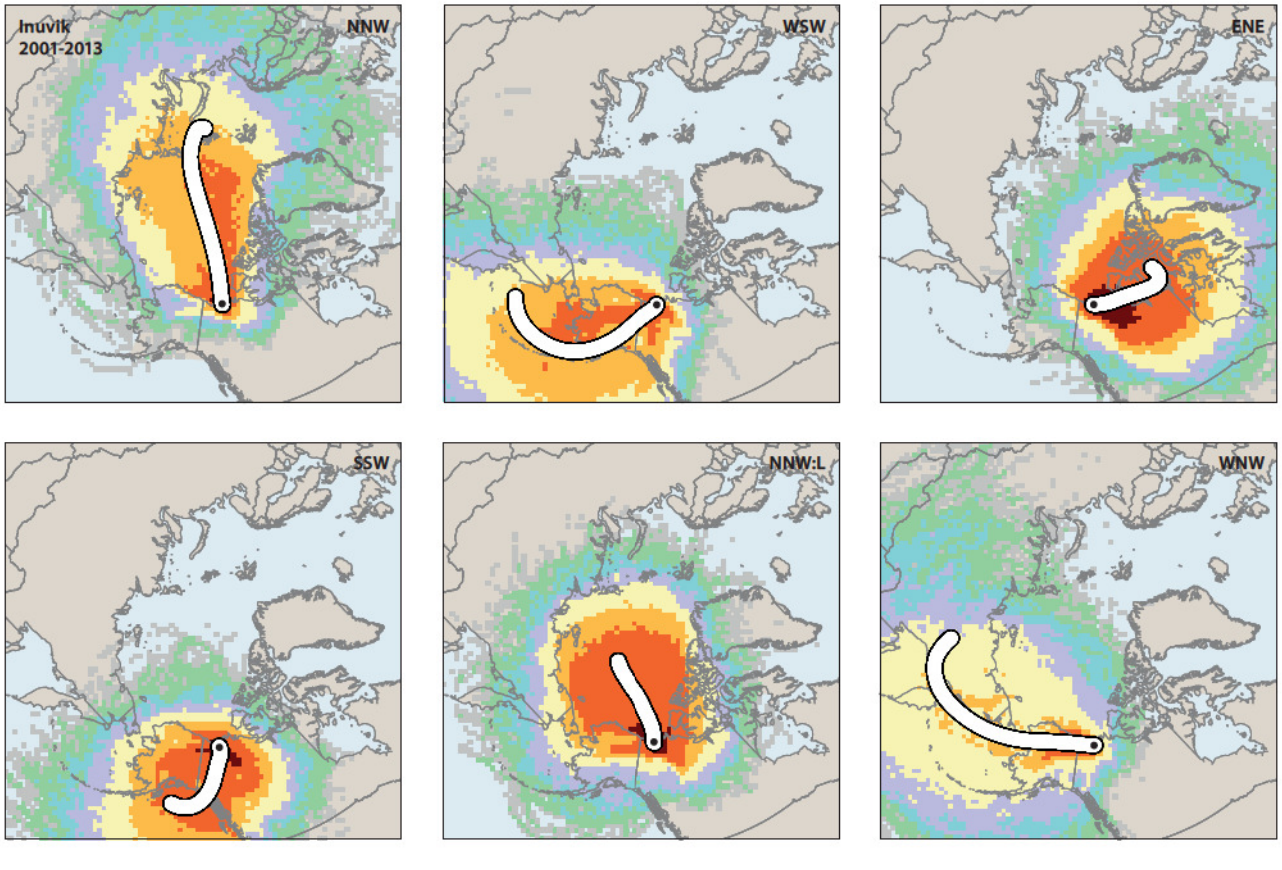

sources from observed atmospheric concentrations using atmospheric transport models, if the monitoring network is sufficiently dense. With the increase in Arctic monitoring of methane over the past few years, it is possible to start to identify the regions which contribute most strongly to atmospheric concentrations observed at these sites. The next step is to scale up this information to estimate source strength for a given spatial area, however, that requires a full atmospheric transport modelling approach and is explored in more detail in Ch. 7. The analysis presented here provides the context for that investigation.

Temporal variability in synoptic weather patterns leads to specific regional-scale transport pathways that can significantly affect concentrations over downwind locations. The magnitude of this effect depends upon the magnitude of upwind emissions and the rate of transport of the air mass. Several techniques have been used to study how atmospheric concentrations differ with transport path, but the majority of approaches tend to utilize back-trajectories to characterize the transport. Overall, more meaningful conclusions can be drawn when atmospheric concentrations are examined in relation to ensembles or large groupings of trajectories, as opposed to individual trajectories. Here, a trajectory cluster analysis has been applied to nine Arctic monitoring sites with continuous hourly-averaged data, to determine which upwind areas tend to lead to higher and/or lower observed methane concentrations. These regions can then be examined for their correspondence to known natural or anthropogenic methane sources present in these regions.

The type of trajectory cluster analysis used here has also been used in other studies to create ensembles of trajectories or 'trajectory clusters' with common transport pathways (Dorling and Davies 1992; Dorling et al. 1992; Chan and Vet 2010). The ensembles or clusters determined through this approach reflect typical meteorological patterns in the area around the receptor sites. Six different clusters were determined to be sufficient to differentiate the main transport patterns.

A detailed example of the trajectory cluster analysis for Inuvik (Canada), a regionally-influenced site in the proximity of extensive wetland regions, is shown in Fig. 6.10. The annual methane cycles at Inuvik were examined according to the six main transport pathways (see upper left plot of Figure 6.10). The methane observations at Inuvik are linked with source regions covering air flow up to ten days back in time (the six upper right panels). Clear evidence of a secondary summer peak is observed from the western (WNW and WSW) clusters where transport over known wetland regions has occurred. In contrast, for the clusters originating from the Arctic Ocean to the north and north-east (NNW and ENE), secondary peaks in the annual methane cycle are much less obvious, clearly showing the impact of methane emissions from wetlands in the region. The centre panel of Fig. 6.10 shows the four seasonal box-and-whisker methane plots for the Inuvik site. This provides a measure of the variability observed by cluster and by season.

Figure 6.11 shows the mean annual methane cycle according to transport pathways for the other eight sites included in the analysis. The method used is to establish climatologically, the synoptic flow patterns associated with these sites. The endpoint for the vectors shown represents the mean upwind distance ten days back in time. Shorter vectors thus indicate slower travel speed and possible stagnation along the path while longer vectors are related to stronger wind speeds. The percentage of trajectories for a given cluster is shown on the endpoint of the mean vector. The direction labelled with 'L' represents a lighter (slower) transport speed relative to the other cluster from the same direction. Similar to Inuvik (Canada), the sites exhibit various magnitudes in the summer secondary peak, contingent on transport direction. Barrow (Alaska, USA) shows a small enhancement in summer methane concentration for air masses originating from the SSW and SSE sectors, relative to the ocean clusters to the north. At Behchoko (Canada), enhancements are found from the two western clusters while at Churchill (Canada) more obvious enhancements in summer methane concentration are associated when air masses originate from the WNW, WNW:L and WNW:L2 clusters. Slightly further south in central Alaska, the CARVE site shows some evidence of a summer peak from the WNW and WNW:L clusters, but these are not nearly as pronounced as those observed at the other high latitude North American sites (such as Churchill).

On the other side of the Arctic landmass, the clustered annual methane concentrations at Tiksi and Cherskii (Russia) also show distinctly different annual cycles associated with the transport of air masses originating from land clusters relative to ocean clusters. The amplitude of the summer peak for land clusters is more pronounced at these two sites than that observed at any of the North American sites, possibly suggesting a closer proximity to more extensive wetland emission sources. In contrast, sites located far from wetland sources (i.e. Alert, Canada) do not appear to show secondary summer peaks associated with any transport direction.

At Pallas (Finland), methane concentrations originating from the south are significantly enhanced throughout the year compared to other transport directions. This is likely to be due to the transport of methane from both anthropogenic and wetland emission sources in the mid-latitudes.

6.5 Methane measurements at Tiksi on the coast of the Laptev Sea

Observations of methane concentration at Tiksi (Russia) were initiated in July 2010 to aid in understanding terrestrial emissions from the Siberian tundra and marine emissions from the shallow Laptev and East Siberian Seas, which are known for methane hydrate deposits in the seabed and oversaturated seawater methane concentrations (Shakhova et al. 2010). The Tiksi monitoring station is operated by the Yakutian hydrometeorological service, and measurements are conducted through co-operation between the Finnish Meteorological Institute, the US National Oceanic and Atmospheric Administration, the Arctic and Antarctic Research Institute and the Voeikov Main Geophysical Observatory (St. Petersburg). The city of Tiksi (about 5000 inhabitants) is located on the coast of the Laptev Sea and within several hundred kilometers of both the Lena River and an extensive wetland area (~300,000 km^2). The city is approximately 5 km north of the measurement location.

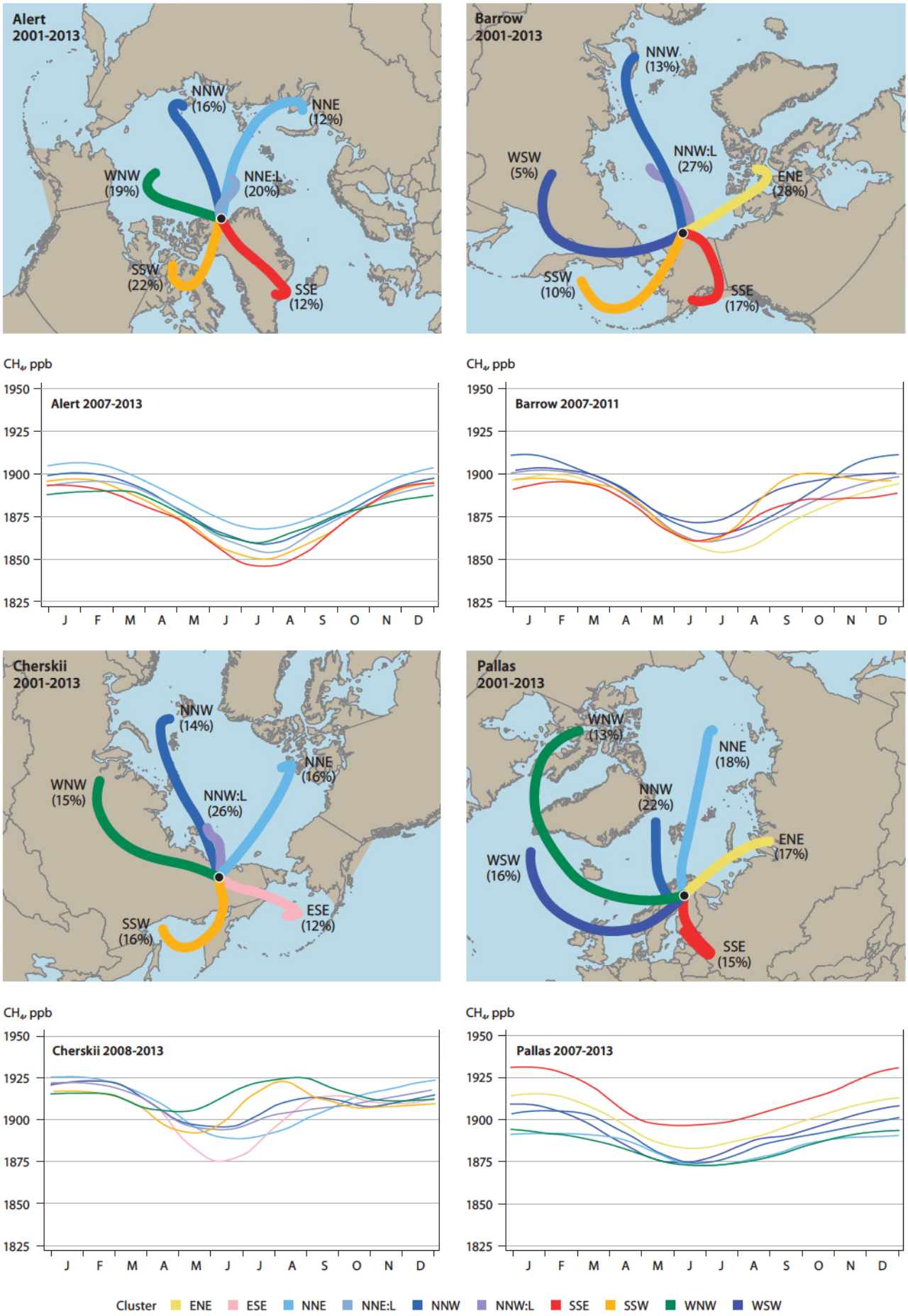

Fig. 6.11 Trajectory cluster mean vectors at eight high-latitude sites with continuous methane measurements. Six trajectory clusters were sorted by the k-means clustering technique similar to that of Chan and Vet (2010) using Euclidean distance as the dissimilarity metric on 10-day air parcel backward trajectories from 2001 through 2013 for all sites.

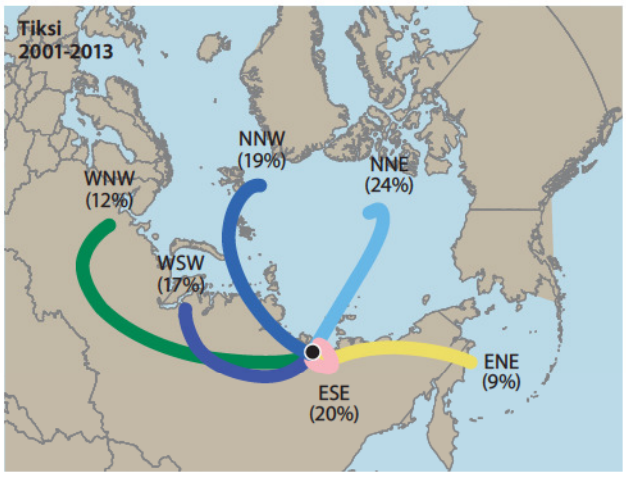
Tiksi
2001-2013
WNW
(12%)
NNW
(19%)
NNE
(24%)
WSW
(17%)
ENE
(9%)
ESE
(20%)

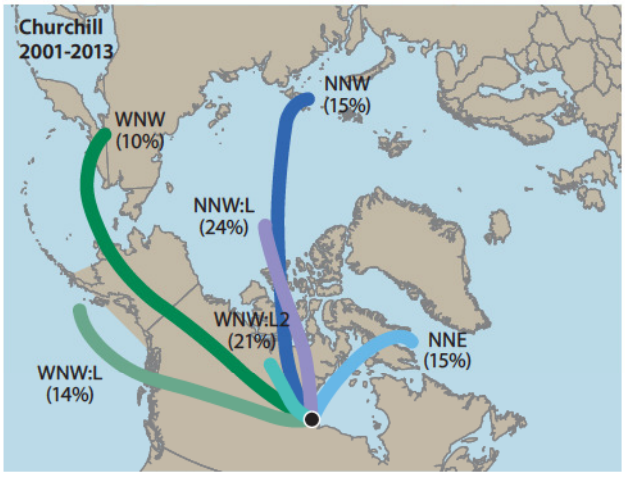
Churchill
2001-2013
WNW
(10%)
NNW
(15%)
NNW:L
(24%)
WNW:L2
(21%)
NNE
(15%)
WNW:L
(14%)

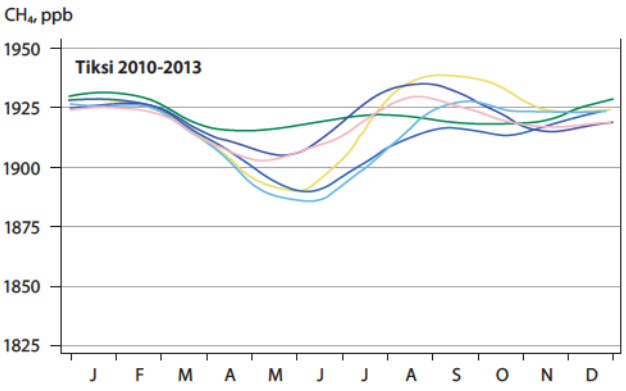
CH4, ppb
Tiksi 2010-2013
1950
1925
1900
1875
1850
1825
J F M A M J J A S O N D

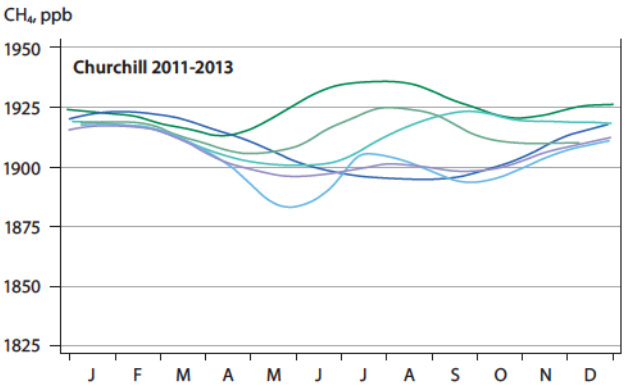
CH4, ppb
Churchill 2011-2013
1950
1925
1900
1875
1850
1825
J F M A M J J A S O N D

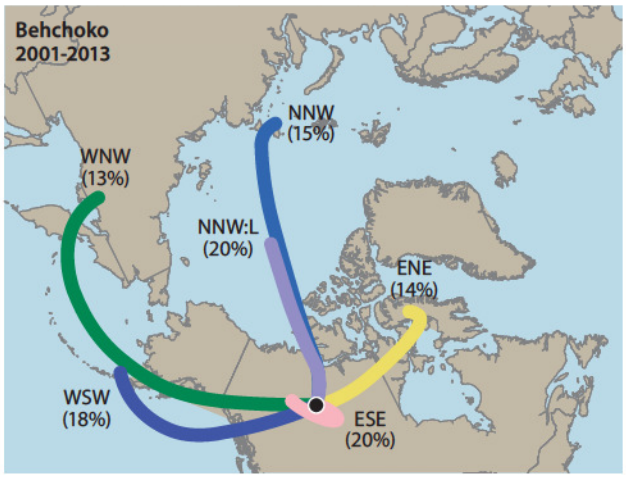
Behchoko
2001-2013
WNW
(13%)
NNW
(15%)
NNW:L
(20%)
ENE
(14%)
WSW
(18%)
ESE
(20%)

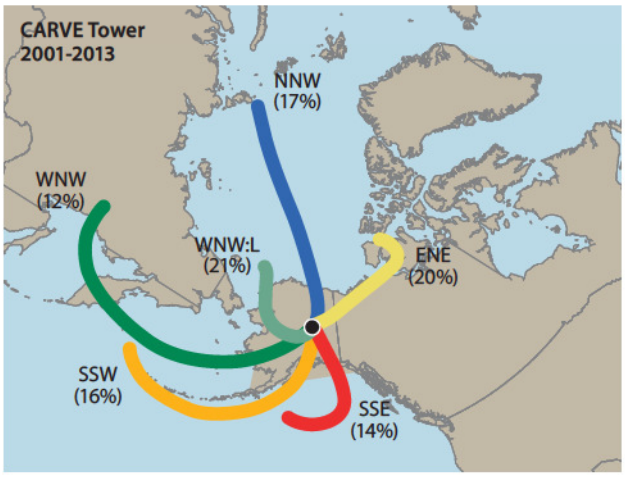
CARVE Tower
2001-2013
NNW
(17%)
WNW
(12%)
WNW:L
(21%)
ENE
(20%)
SSW
(16%)
SSE
(14%)

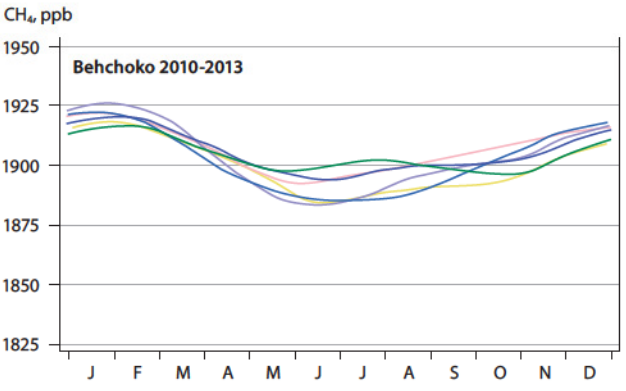
CH4, ppb
Behchoko 2010-2013
1950
1925
1900
1875
1850
1825
J F M A M J J A S O N D

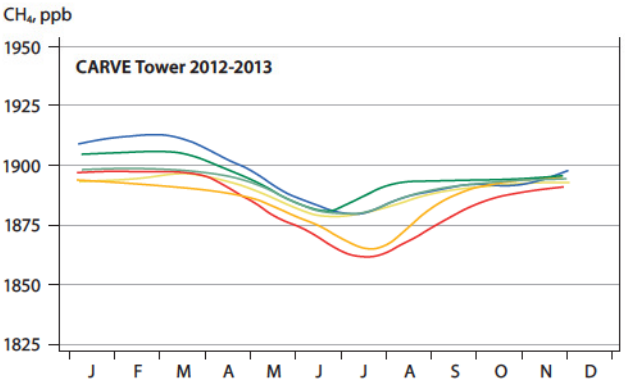
CH4, ppb
CARVE Tower 2012-2013
1950
1925
1900
1875
1850
1825
J F M A M J J A S O N D

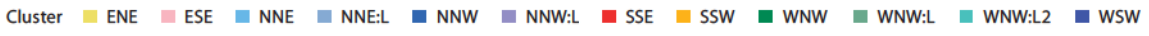
Cluster
ENE
ESE
NNE
NNE:L
NNW
NNW:L
SSE
SSW
WNW
WNW:L
WNW:L2
WSW

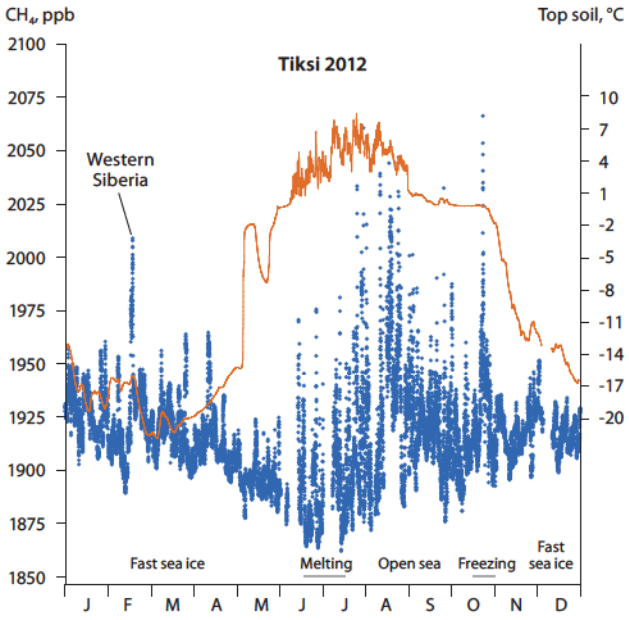

Fig. 6.12 Half-hourly averaged methane concentrations at the Tiksi monitoring station (Russia) on the Laptev Sea coast through 2012. Surface soil (5cm) temperature and sea-ice conditions for the Laptev Sea ice are also shown.

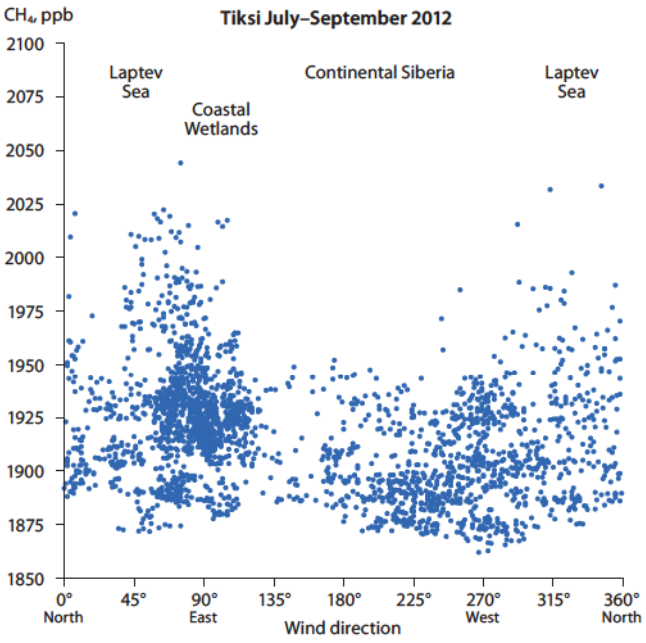

Fig. 6.13 Half-hourly averaged methane concentrations (July–September 2012) relative to wind direction at the Tiksi monitoring station (Russia) on the Laptev Sea coast. Observations are only included if wind speed is greater than 3 m/s, because wind direction is not well developed when wind speed is low.

The annual cycle of atmospheric methane (see also Sect. 6.4.2) reflects winter emissions from industrial sources in the western and southern parts of Siberia. In summer, the Laptev Sea is ice-free from early July to mid-October, indicating the potential presence of marine methane emissions. This is roughly the same period as when the terrestrial surface active layer in the tundra has thawed and methane production takes place. Elevated methane concentrations during this period are apparent (Fig. 6.12). Methane increased during calm nights, indicative of local tundra emissions (and this was confirmed by the micrometeorological method – not shown). On average, ambient methane levels at Tiksi are higher than at other High Arctic sites because of extensive Siberian wetland emissions and often limited vertical mixing in the stable shallow atmospheric boundary layer.

To evaluate the potential emission intensity around the Tiksi site, half-hourly average methane concentrations were plotted relative to wind direction during the main open water period for the Laptev Sea and the terrestrial active season (Fig. 6.13). Methane concentrations (when low wind speed cases are excluded) were between 1870 ppb (background level) and 2050 ppb (the highest concentration). As a generalization, methane concentrations did not appear to reflect wind direction. The lack of elevated concentrations when winds are from the south and southwest sectors may be because uplands and the Verhoyansk Mountains are in that direction. The highest concentrations observed when the wind direction was from the Laptev Sea sector were relatively modest, which does not indicate extensive emissions in that area. Concentrations were slightly elevated when winds were from the eastern sector, where widespread coastal wetlands occur. Trajectory analysis (see Sect. 6.4.3; Fig. 6.11) also confirms elevated concentrations when air masses originate from the east.

6.6 Isotopic measurements

Atmospheric monitoring of methane isotopes – primarily $\delta^{13}C_{CH4}$ – in ambient air, coupled with trajectory analysis, can help distinguish the contribution of specific source types to atmospheric methane concentrations. For reference, background ambient air has a $\delta^{13}C_{CH4}$ value of around -47.3‰ in the northern hemisphere and -46.9‰ south of the Inter-Tropical Convergence Zone. Deviations from the background level can be used to identify sources of methane present in Arctic air, which can be either enriched or depleted in ^{13}C depending on the formation process. Different sources of carbon have different signatures of ^{13}C, which are often referred to as isotopic fingerprints (Table 6.2). Biogenic sources are relatively depleted in ^{13}C (also referred to as 'light'), and thermogenic sources are relatively enriched in ^{13}C (also referred to as 'heavy'), in comparison to background air. For example, wetlands emit methane with $\delta^{13}C_{CH4}$ around -70±5‰, depending on location, meteorology and local species composition in the wetlands (e.g. dominance of *Eriophorum* cottongrass or *Sphagnum* mosses), while methane from gas exploration emits methane with $\delta^{13}C_{CH4}$ from -35±10‰ to -55±10‰ depending on the reservoir. Methane from biomass burning can also have a large impact as this source is quite 'heavy', $\delta^{13}C_{CH4}$ about -28‰, relative to other sources.

6.6.1 Available data

Routine monitoring of $\delta^{13}C_{CH4}$ to high precision (around 0.04–0.07‰) is taking place at Cold Bay (Alaska; 55.2°N, 162.7°W), Barrow (Alaska; 71.3°N, 156.6°W), Alert (Nunavut, Canada; 82.4°N, 62.5°W), Ny Ålesund (Svalbard, Norway; 78.9°N, 11.9°E), Pallas (Finland; 68.0°N, 24.1°E) and Kjolnes (Norway; 70.5°N, 29.1°E). Measurements at these stations sample the marine boundary layer except for Pallas, where the samples are inland from central northern Scandinavia. Samples are collected

Table 6.2 $^{13}C_{CH4}$ Isotopic ratios for Arctic methane sources. Based on Dlugokencky et al. (2011), Fisher at al. (2011), Sriskantharajah et al. (2012), Nisbet (2001), Walter et al. (2006), Kirschke et al. (2013) and unpublished data supplied by Royal Holloway, University of London (RHUL) and Environment Canada.

Source	$\delta^{13}C_{CH4}$ ‰
Coal and industry, Europe	-35 ± 10
Natural gas, UK North Sea	-35 ± 5
Natural gas, Siberia (exported to EU)	-50 ± 5
Natural gas, Alberta/BC	-55 ± 10
Ruminants, C4 diet	-50 ± 5
Ruminants, C3 diet	-70 ± 5
Arctic wetlands, Finland	-70 ± 5
Boreal wetlands, Canada	-65 ± 5
Biomass burning, boreal vegetation	-28 ± 2
Landfills, Europe	-57 ± 4
Thermokarst lakes	-58 to -83
Hydrates, Arctic	-55 ± 10

weekly or twice weekly at Cold Bay, Barrow, Alert, Ny Ålesund and Pallas, and are analyzed at the University of Colorado by INSTAAR (Institute of Arctic and Alpine Research) for NOAA.

Royal Holloway, University of London (RHUL) also analyzes samples from Ny Ålesund (daily Mon-Fri); Alert (weekly), Pallas (weekly) and Kjolnes (weekly). Results for Alert and Ny Ålesund (unpublished) analyzed by RHUL are closely comparable to the INSTAAR data and show the same amplitude of the seasonal cycle, which provides confidence that observations from different sites and laboratories can be combined to investigate pan-Arctic characteristics.

In addition to the in situ data, aircraft data are also available. The UK MAMM project (Methane and other greenhouse gases in the Arctic – measurements, process studies and modelling) supports flights from Sweden to Spitzbergen, collecting air at various altitudes along the flight path. In particular, the aircraft searches for air masses that have come from northern European Russia and northern Siberia, as well as occasionally sampling air that in part has come from the east Siberian Arctic shelf. Trajectory analysis is used prospectively and retrospectively to identify source regions for the sampled air. Other aircraft data include those from the NOAA/ESRL Cooperative Network sites, as well as survey flights undertaken as part of the NASA Carbon in Arctic Reservoirs Vulnerability Experiment (CARVE) http://science.nasa.gov/missions/carve/.

6.6.2 Annual cycle

There is clear seasonality in $\delta^{13}C_{CH4}$ in the Arctic, and this is apparent in Figs. 6.14 and 6.15 which show the NOAA/INSTAAR high precision $\delta^{13}C_{CH4}$ measurements for 2000–2012 at four Arctic monitoring stations. An additional non-Arctic measurement site (Mace Head, Ireland) is included for reference. Isotopic measurements become 'heavier' (less negative) in winter, peaking around the time of the spring melt, and then, after melting, shifting to become significantly 'lighter' (more negative) in summer, to reach a minimum $\delta^{13}C_{CH4}$ in autumn. The amplitude of the seasonal $\delta^{13}C_{CH4}$ cycle appears to have increased over time, and in recent years is of the order of 1‰ or more. Globally, the seasonality in $\delta^{13}C_{CH4}$ increases with latitude and is most pronounced in the Arctic, where the OH sink is limited, especially in winter.

The seasonality of $\delta^{13}C_{CH4}$ is systematically offset (i.e. out of sync) from the seasonality in methane concentration, which peaks in late autumn or early winter, some months before the isotopic peak. Concentration minima typically occur in June or July. This offset between atmospheric methane concentration and the isotopic cycle suggests that there is a major 'light' (i.e. biogenic) source that inputs methane to Arctic air from July to October. Another factor that influences the cyclicity, both in methane concentration and isotope fractions, is atmospheric mixing

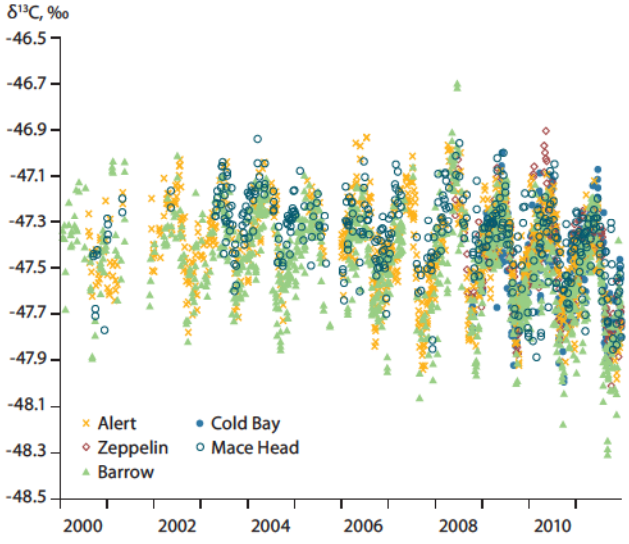

Fig. 6.14 Multi-site NOAA/INSTAAR high precision $\delta^{13}C_{CH4}$ measurements for 2000 through 2012 at the following monitoring stations: Cold Bay (USA), Barrow (USA), Alert (Canada), Ny Ålesund/ Zeppelin (Norway) and Mace Head (Ireland).

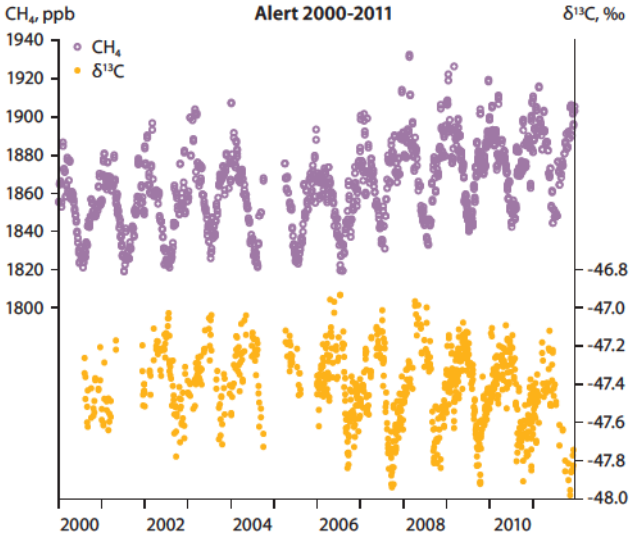

Fig. 6.15 Detail of Arctic NOAA/INSTAAR results from Alert (Canada): (upper) methane concentrations and (lower) methane isotope ($\delta^{13}C_{CH4}$) record.

with background Atlantic and Pacific air from lower latitudes. This may contribute to the concentration decline in spring, OH destruction, which in May-July will reduce concentrations and drive $\delta^{13}C_{CH4}$ 'heavier'. Also stratospheric inputs via episodes of polar vortices, may similarly reduce methane concentration and drive an increase in $\delta^{13}C_{CH4}$, especially in winter.

6.6.3 Identification of Arctic methane sources

Fisher et al. (2011) found that the bulk Arctic methane source signature for air arriving at Spitzbergen in late summer 2008 and 2009 was about $\delta^{13}C_{CH4}$ -68‰. The source signature of methane in these samples had $\delta^{13}C_{CH4}$ -68.6±4.5‰ in July 2009 and $\delta^{13}C_{CH4}$ -68.7±4.4‰ in October 2010. Air sampled daily at Ny Ålesund in September–October 2009 had a source signature of $\delta^{13}C_{CH4}$ -67.4±3.1‰. Recent unpublished work by RHUL in collaboration with the Norwegian Institute for Atmospheric Research and with the MAMM project showed very similar results, which clearly reflect an Arctic wetland source (see Table 6.2). In contrast, also at the Ny Ålesund station, Fisher et al. (2011) found that in March to May 2009 (when wetlands are frozen), the small Arctic springtime source, calculated from measurements in air samples collected daily, was $\delta^{13}C_{CH4}$ -52.6±6.4‰. Although the precision of this determination is poor, this bulk Arctic source signature closely matches Russian Arctic gas supplies (Dlugokencky et al. 2011) (see Table 6.2). Stratospheric air measured over Finland (RHUL, unpubl.) may also contribute to the decline in mixing ratios during spring while $\delta^{13}C_{CH4}$ increases. More recent studies by RHUL, including airplane transects, have confirmed both the spring and high summer findings of Fisher et al. (2011).

The isotopic results to date, imply that methane emitted in the Arctic, over and above the seasonal background in maritime air entering from further south, is dominated by wetland emissions in summer and a much smaller fossil fuel source in winter. It is possible that the amplitude of the isotopic seasonality may be increasing, which perhaps suggests that wetland emissions are increasing. This is consistent with Arctic warming if emissions of methane from wetlands (methanogenic flux) increase exponentially with temperature, although methane consumption (methanotrophy) would also be expected to increase (see Ch. 3 and 4).

There has been much debate about the possibility of significant methane release from methane hydrates in the Arctic Ocean as temperatures rise (Nisbet 1989; Archer et al. 2009). In particular, large fluxes have been estimated by upscaling emissions measured from the eastern Siberian Arctic Shelf (Shakhova et al. 2010) and there is clear evidence for submarine bubble plumes (Westbrook et al. 2009), although these methane bubbles do not necessarily reach the sea surface (see Ch. 4). The isotopic results of Fisher et al. (2011) and unpublished data from the MAMM campaign suggest that methane hydrates are not currently a major source of atmospheric methane. Although isotopic values in hydrates can vary greatly, most Arctic hydrates have a $\delta^{13}C_{CH4}$ of around -55±10‰ (Milkov et al. 2005; Fisher et al. 2011) (see Table 6.2). If such comparatively 'heavy' hydrate-sourced fluxes contributed substantially to the approximately -53‰ late winter/spring Arctic methane increment reported by Fisher et al. (2011), then that same signal would be expected, at least to some extent, to affect summer Arctic methane observations. However, this has not yet been observed. To determine source contributions with certainty, additional measurements are required, as well as transport modelling.

6.7 Conclusions

6.7.1 Key findings

The recent expansion of Arctic methane measurements has enabled improved characterization of daily, seasonal and interannual variations in atmospheric methane levels at the local and regional scale. Overall, there has been an increase in atmospheric methane abundance since measurements began, despite some interannual variability. Since 2008, the mean Arctic atmospheric methane concentration has been increasing at about the global rate, ~6 ppb/y (2008–2013). From these measurements, it is evident that in winter, regionally influenced sites are impacted by transport from mid-latitude source regions while in summer, there is considerable variability due to strong diurnal cycles. Before calculating seasonal cycles and long-term trends, it is important to separate out the impacts of localized diurnal variability so that any subsequent analysis is performed on data that are more representative of large, well-mixed volumes of the troposphere. The annual cycle at remote background sites shows a minimum in methane concentration in July/August and a maximum in February. The annual cycle at regionally and locally influenced sites also show a maximum in February as well as a secondary peak in methane concentration in late summer. This secondary peak is likely to be due to the advection of air with enhanced methane levels due to emissions from wetland areas.

Methane isotopic data from Arctic measurement sites provide additional evidence that summer atmospheric concentrations are dominated by contributions from wetlands sources, and in winter by local and regional fossil fuel sources.

There is general concern that Arctic ecosystems may undergo significant changes if Arctic warming trends continue. This is especially true for methane since existing and potential natural Arctic methane sources are large and widespread (i.e. wetlands and marine methane hydrates). The climate feedback from such changes could potentially be very large although, to date, no definitive changes in Arctic methane emissions have been detected by the existing observational network.

An important goal of international observational programs is to provide high quality data to support the characterization of regional-scale information on greenhouse gases. One capability of such programs is the ability to infer emissions from anthropogenic source sectors. With the improved availability of long-term, high time resolution methane observations and coincident improvements in modelling capability (see Ch. 7 and 8), it will eventually become possible to track regional emissions of methane, including those from fossil fuel use, agriculture and waste over long periods. Equally important will be the ability to utilize long-term observations to evaluate observational constraints on large-scale emissions and sinks, and to improve understanding of the carbon cycle for large ecosystems such as tundra and high boreal forest regions, an approach which is detailed in Ch. 7.

6.7.2 Recommendations

The data presented in this chapter have the potential to identify and locate major sources of Arctic methane by type and seasonality. However, continuity in long-term data records for both weekly and hourly measurements is essential to support this work. Integration of the long-term observational data (including isotopic measurements) with short-term airborne measurements and data from ground-based remote sensing platforms would provide a more accurate representation of the true spatial and temporal gaps in the observing system. This analysis should be completed as a next step. Subsequently, and as modelling capabilities continue to evolve, a detailed assessment of the adequacy of the observational network to detect future atmospheric change and to support the characterization of sources may be warranted. Ensuring the timely availability of both short- and long-term observational data to support future analyses is critical to ensuring a full understanding of the limitations of the current observing system. Common data archiving and quality control/assurance practices would also improve data inter-comparability.

Finally, maintaining the existing long-term data records, as well as continuing to evaluate the spatial and temporal coverage of Arctic atmospheric methane measurements is an essential component in improving the ability to assess the overall impact of regional and global methane sources, as well as to assess the response of the Arctic to climate change.

Acknowledgments

Authors are grateful for valuable comments and suggestions on earlier drafts of this chapter provided by Pieter Tans.